Facile One-pot Preparation of Novel Shell Cross-linked Nanocapsules: Inverse Miniemulsion RAFT Polymerization as an Alternative Approach

Yin Wang[a,b], Guohua Jiang[*a,b], Ming Zhang[a], Lina Wang[b], Rijing Wang[a,b] and Xinke Sun[a,b]

[a]*Key Laboratory of Advanced Textile Materials and Manufacturing Technology (Ministry of Education),Zhejiang Sci-Tech University, Hangzhou 310018, China*

[b]*Department of Materials and Technology, College of Materials and Textiles, Zhejiang Sci-Tech University, Hangzhou 310018, China*

---

[*] To whom correspondence should be addressed. Tel: +86 571 86843527; E-mail address: polymer_jiang@hotmail.com (G. Jiang).

The mechanism for synthesis of shell cross-linked PDMAEMA-*b*-PMAA nanocapsules *via* inverse miniemulsion RAFT polymerization

Inverse miniemulsion RAFT polymerization has a combine mechanism of inverse miniemulsion polymerization and RAFT polymerization. Stabilized oil droplets with monomers located in cores were prepared by soncating the coarse inverse emulsion. Then the polymerization was initiated by APS at 60 $^{\circ}$C, the monomers would transfer outside and insert between PDMAEMA blocks and -S-C(=S)-S- groups. That is PDMAEMA would have a chain extension by MAA. So after a period time, the resultant nanocapsules would have a core-shell structure, with PDMAEMA as cores and cross-linked PMAA as shells. The illustrated mechanism is demonstrated in Scheme S1.
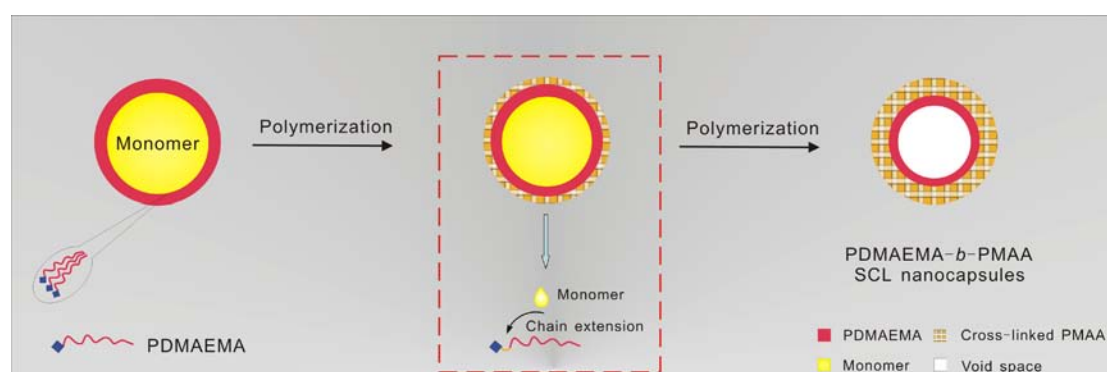
Scheme S1 The illustrated mechanism for the fabrication of shell cross-linked PDMAEMA-*b*-PMAA (SCL) nanocapsules *via* inverse miniemulsion RAFT polymerization. The model in the rectangle with red broken line is an intermediate state for synthesis of nanocapsules.

Synthesis of shell cross-linked PDMAEMA-*b*-PMAA nanocapsules *via* inverse miniemulsion RAFT polymerization

FT-IR spectroscopy was employed to characterize the compositions of PDMAEMA,

PDMAEMA-*b*-PMAA nanocapsules and SCL nanocapsules. Fig. S1A is the FT-IR spectrum of PDMAEMA, whose characteristic absorption bands of C-N stretching vibration at 1148 cm^{-1} and C=O stretching vibration at 1726 cm^{-1}. Moreover, the relative intensity of C-N stretching vibration is stronger than that of C=O stretching vibration. Comparing to the PDMAEMA sample, the O-H deformation vibration at 1400.3 cm^{-1}, C=O stretching vibration at 1709.1 cm^{-1} resulted from hydrogen bond interaction can be clearly observed in Fig. S1B, which are the typical absorption bands for PMAA. The absorption band of C-N stretching vibration also appears at 1181.4 cm^{-1} in PDMAEMA-*b*-PMAA nanocapsules sample, indicating a successful chain extension of PDMAEMA. After shell cross-linked reaction, all the characteristic absorption bands both for PMAA and PDMAEMA can still be well detected, but the relatively intensity of two absorption bands at 1709.1 cm^{-1}, 1400.3 cm^{-1} have changed significantly, which is attributed to the relatively amount of C=O increasing by introduction of the cross-linker (Fig. S1C). Furthermore, as for PDMAEMA-*b*-PMAA nanocapsules and SCL nanocapsules, the relative intensity of C=O stretching vibration are both stronger than that of C-N stretching vibration (Fig. S1B and S1C). All above well confirms that the PDMAEMA-*b*-PMAA has been successfully fixed by BAEDS to form shell cross-linked nanocapsules.
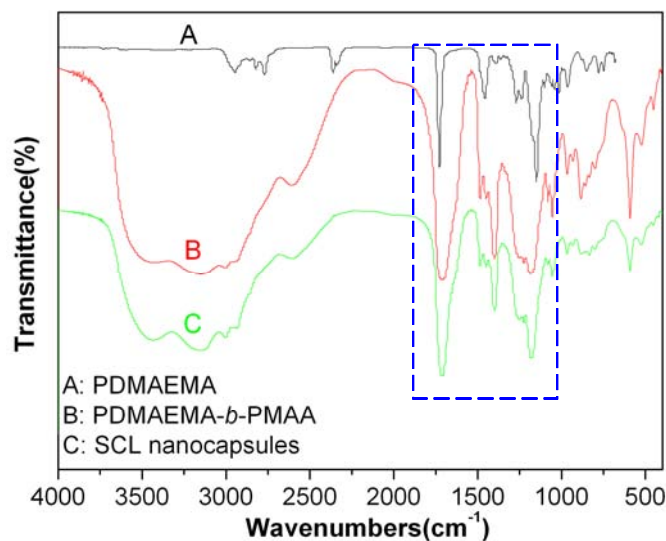
Fig. S1 FT-IR spectra of PDMAEMA (A), PDMAEMA-*b*-PMAA (B) and the SCL nanocapsules (C). PDMAEMA sample was measured by using an ATR cell. The other two samples were measured by using KBr pellets.

The curves of the loss weight rate of the macroinitiators and the resultant nanocapsules in a nitrogen stream from room temperature to 700 ^{o}C were gained by way of TGA. Fig. S2 shows the weight lose curves of PDMAEMA, PDMAEMA-*b*-PMAA, the SCL nanocapsules and NaCl-containing SCL nanocapsules. As it can be seen, the thermal stability of the three polymers is different (A to C). For PDMAEMA, it begins to decompose when the temperature increases to 178 ^{o}C. The sample weight lose is about 50 % when the temperature is reached at 370 ^{o}C, and decomposition almost completely at 450 ^{o}C. In the case of PDMAEMA-*b*-PMAA, four decomposition stages can be observed. Below 100 ^{o}C, the water begins to evaporate from the sample. The second decomposition stage from 100 ^{o}C to 220 ^{o}C is attributed to the bond leakage between PDMAEMA blocks and -S-C(=S)-S- groups. The third decomposition stage is caused by

the decomposition of PDMAEMA whose decomposition temperature is about 280 ^{o}C. The final decomposition temperature is 400 ^{o}C, which is near the initial decomposition temperature of homo-poly (methylacrylic acid). All above indicates that PDMAEMA-*b*-PMAA nanocapsules have been successfully prepared *via* aqueous RAFT polymerization. In addition, it can be seen from Fig. 2C that the weight loss curve of the SCL nanocapsules has shifted to high temperature region, which implies that the sample has an excellent thermal stability after shell cross-linked reaction. Furthermore, the max weight lose temperature below 100 ^{o}C has also shifted to high region (DTG data, which is not shown), indicating that the SCL nanocapsules have impermeable shells. All above further confirms that the shell cross-linked nanocapsules have been successfully fabricated by simply introducing the cross-linker to the inverse miniemulsion RAFT polymerization system.
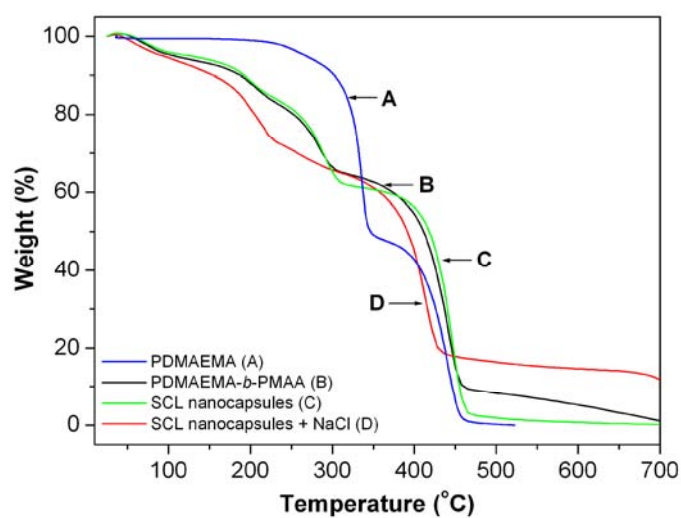

Fig. S2 TGA curves of PDMAEMA (A), PDMAEMA-*b*-PMAA (B), the SCL nanocapsules (C) and NaCl-containing SCL nanocapsules (the amount of NaCl added into the dispersed phase is 0.1 g) (D).

Fig. S3 is the TEM images of NaCl-containing shell cross-linked PDMAEMA-*b*-PMAA nanocapsules. The phenomena are similar to that of Fig. 3. In briefly, spherical nanocapusles with a size of 200-300 nm can be seen and the void space within nanocapsules decreases as the amount of NaCl increases. Besides, the crystal degree is improved gradually as the amount of NaCl increases.
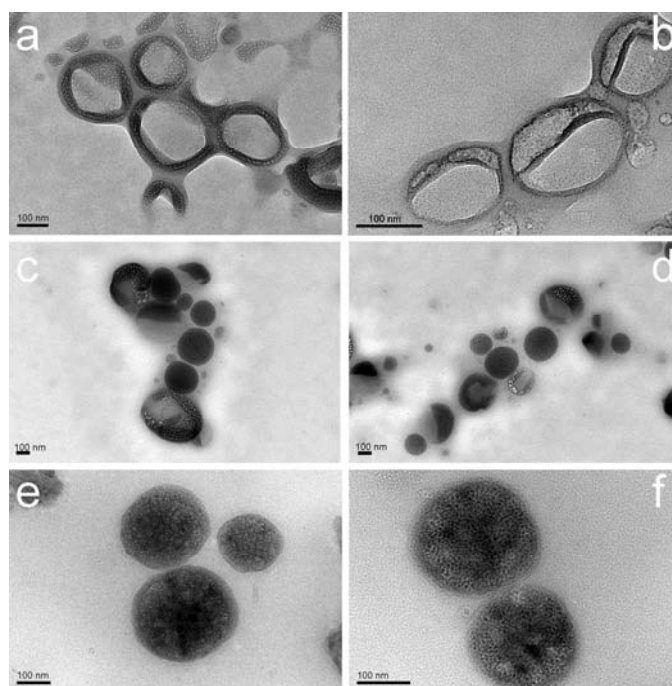

Fig. S3 Representative TEM images of sodium chloride-containing shell cross-linked PDMAEMA-*b*-PMAA nanocapsules. All scale bars are 100 nm. The concentration of the samples is 1 mg/mL. The amount of NaCl added into the dispersed phase is 0.03 g (a, b), 0.05 g (c, d) and 0.1 g (e, f), respectively.

Encapsulation of sodium chloride into shell cross-linked PDMAEMA-*b*-PMAA nanocapsules *via* inverse miniemulsion RAFT polymerization

Different amount of NaCl was successfully encapsulated into SCL nanocapsules *via* inverse

RAFT polymerization. The influences on the nanocapsule size and Span value were investigated by DLS. As shown in Fig. S4, the diameter decreases with a concomitant increase in amount of NaCl. However, the Span value shows a different tendency which decreases firstly, then increases. The reasons are as follows: firstly, it is attributed to the function of NaCl which acts as co-stabilizer to reduce interfacial tension.[1] The more amount of NaCl is, the more stable of the oil droplets are. That is, increasing amount of NaCl would restrict the monomers to diffuse to the continuous phase and prevent small oil droplets to aggregate. So when the amount of NaCl is increases, the diameter of the nanocapsules decreases. Secondly, allowing reaction mixture to precipitate by gravity for a period of time may eliminate the contribution of larger nanocapsules. In addition, it can be seen from the Fig. S4b, increasing the amount of NaCl also has a positive impact on narrowing the variation of Span value. It is consistent with the reported results.[1,2]
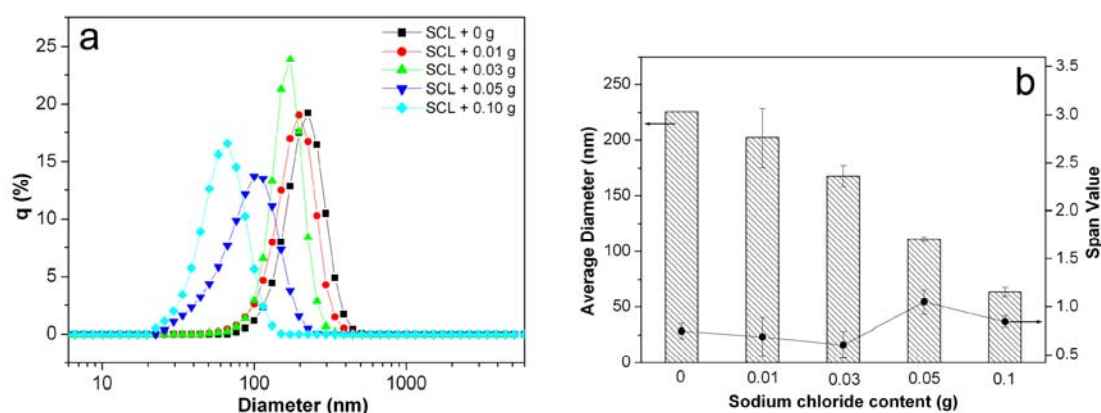

Fig. S4 Dependence of the nanocapsule size and Span value for sodium chloride-containing nanocapsules on different amounts of salt in cyclohexane dispersion at 25 ^{o}C. The concentration of all samples is 1 mg/mL.

The calculated equation:

Distribution span obtained using the equation below: this is not displayed if neither of % on Diameter is specified.

$$\text{Span value} = (\text{Diameter on \% A} - \text{Diameter on \% B}) / \text{Median} \qquad (1)$$

Where, Diameter on % A: First value to be entered in Display Condition; Diameter on % B: Second value to be entered in Display Condition; Median: Particle size equivalent to cumulative 50 %.[3]

EDXA was used to investigate the sample compositions of NaCl-containing SCL nanocapsules. The spectrum shows that the presence of carbon (C), oxygen (O) and sulfur (S) in the sample (Cu from the copper EM grid and Cr from the specimen holder of TEM). Besides, evidence of sodium (Na) and chlorine (Cl) can also be clearly seen in Fig. S5, which indicates that NaCl has been successfully encapsulated into SCL nanocapusles. TGA analysis further confirms that the weight percentage of encapsulated NaCl is 14 % (Fig. S2D).
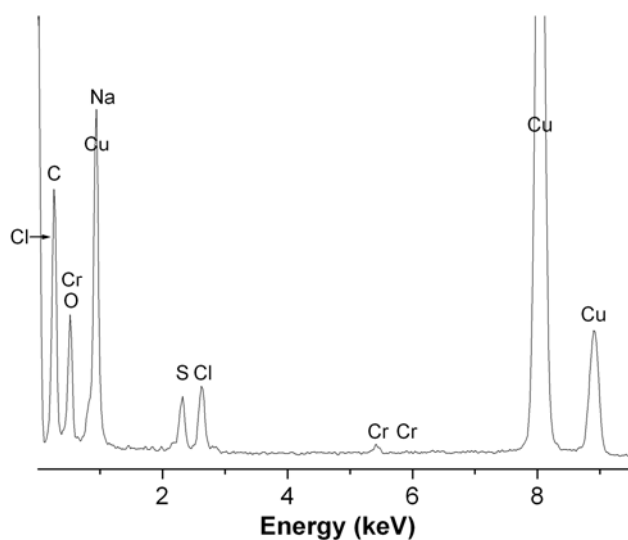

Fig. S5 EDXA spectrum of NaCl-containing SCL nanocapsules.

Fig. S6 is the electrical diffraction of NaCl with a low crystal degree. It can be found that the electrical diffraction is not as obvious as that of displayed in Fig. 3d, which indicates that the crystal degree of NaCl is relatively low.
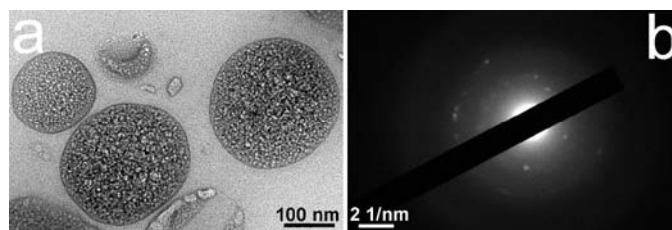

Fig. S6 TEM electrical diffraction of NaCl with a low crystal degree encapsulated in SCL nanocapsules. The amount of NaCl added into the dispersed phase for Fig. S6a is 0.05 g.

Notes and references

[1] E. Kobitskaya, D. Ekinci, A. Manzke, A. Plettl, U. Wiedwald, P. Ziemann, J. Biskupek, U. Kaiser, U. Ziener and K. Landfester, *Macromolecules*, 2010, **43**, 3294-3305.

[2] Z. H. Cao, U. Ziener and K. Landfester, *Macromolecules*, 2010, **43**, 6353-6360.

[3] The equations to calculate Span value and Median are derived from the LB-550 Operation section of the handbook supplied by HORIBA (Pagell-15, 16).